Assessing the artificial radionuclide Cesium-137 spatial distribution in the Southern Hemisphere from lake sediment records

Floriane Guillevic, Pierre Sabatier, Gerald Dicen, Palak Aggarwal, Anthony Foucher, Olivier Evrard, Christine Alewell

Journal of Environmental Radioactivity 293 (2026) 107906

Contents lists available at ScienceDirect

Journal of Environmental Radioactivity

journal homepage: www.elsevier.com/locate/jenvrad

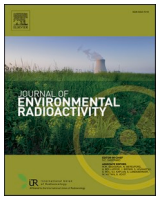

Assessing the artificial radionuclide Cesium-137 spatial distribution in the Southern Hemisphere from lake sediment records

Floriane Guillevic [a,*], Pierre Sabatier [b], Gerald Dicen [a,d], Palak Aggarwal [a], Anthony Foucher [c], Olivier Evrard [c], Christine Alewell [a]

[a] Environmental Geosciences, Department of Environmental Sciences, University of Basel, Basel, CH-4056, Switzerland
[b] EDYTEM, Université Savoie Mont-Blanc, Université Grenoble Alpes, CNRS, Le Bourget du Lac, 73376, France
[c] Laboratoire des Sciences du Climat et de l'Environnement (LSCE/IPSL), UMR 8212 (CEA/CNRS/UVSQ), Université Paris-Saclay, Gif-sur-Yvette, 91191, France
[d] Department of Science and Technology-Philippine Nuclear Research Institute (DOST-PNRI), Commonwealth Avenue, Diliman, 1101, Quezon City, Philippines

ARTICLE INFO

Keywords:
^{137}Cs activity peak
^{137}Cs profile
Environmental parameters
Latitude –southern hemisphere

ABSTRACT

When supported by a reliable geochronology, lake sediments provide important archives for environmental and climatic changes. Artificial radionuclides in general, and cesium-137 (^{137}Cs) in particular, are frequently used to validate sediment chronologies over the past century. This review and meta-analysis assessed the spatial distribution and variability of ^{137}Cs in lake records from the Southern Hemisphere, while also identifying geographical data gaps. The ^{137}Cs profile shapes and inventories were compared and categorized, and their relationships with environmental variables were tested. The spatial distribution of available data reveals an imbalance in studies available across the Southern Hemisphere, with South America showing the greatest research coverage. While the sedimentation rate was identified as a key factor of ^{137}Cs variability, two groups identified from the database presented high peak activities regardless of sedimentation rate, particularly in lakes located between 40°S and 50°S in Chile and Argentina. Lake geographic location (and their distance from nuclear test sites) appears to be the most influential factor explaining disparities in ^{137}Cs deposition. Surprisingly, neither precipitation nor lake elevation showed a significant correlation with ^{137}Cs peak activity.

1. Introduction

Reliable time markers are essential for reconstructing environmental changes over the past century, as these shifts have negatively impacted soils, surrounding waters, and ecosystems, particularly in the Southern Hemisphere (Hancock et al., 2011; Zalles et al., 2021). For nearly five decades, artificial radionuclides have been extensively used as effective time markers/geochronometers to document a variety of environmental changes (Appleby, 2001; Pennington et al., 1973; Ritchie et al., 1973; Ritchie and McHenry, 1990).

The artificial radionuclide cesium-137 (^{137}Cs, $t_{1/2}$ = 30.2 years) is commonly used to independently validate sediment chronologies in lakes based on the naturally-occurring radionuclide lead-210 (^{210}Pb, $t_{1/2}$ = 22.2 years) and its atmospherically supplied (excess ^{210}Pb) fraction (Bruel and Sabatier, 2020). More recently, the use of the isotopes ^{240}Pu and ^{239}Pu has increased to refine sediment chronologies and offer an additional tool to complement ^{137}Cs (Ketterer et al., 2004; McCarthy et al., 2023; Röllin et al., 2022; Zhao et al., 2025). However, the application of ^{240}Pu and ^{239}Pu isotopes in lake sediments remains limited in the Southern Hemisphere (SH) with very few studies so far (Chaboche et al., 2022; Hancock et al., 2011; Sanders et al., 2017). Therefore, ^{137}Cs continues to be the primary artificial radionuclide for validating lake sediment records globally.

In the Northern Hemisphere (NH), particularly in Europe, the distribution of ^{137}Cs is relatively well-documented. Sediment cores commonly show one or two distinct peaks in ^{137}Cs activity. The first peak in ^{137}Cs activity corresponds to the year of maximum fallout in the Northern Hemisphere in 1963 CE, which marked the end of nuclear bomb tests by the former Soviet Union and the USA. The second peak of ^{137}Cs activity is associated with the Chernobyl nuclear power plant accident, which occurred in 1986 CE (Foucher et al., 2021), and which generated fallout across wide regions in Europe (Meusburger et al., 2020). In the Southern Hemisphere (SH), global fallout was also widely distributed after 1963. Notably, France continued atmospheric thermonuclear bomb testing at Mururoa and Fangataufa atolls in French Polynesia (22° S) between 1966 and 1974, contributing to additional

* Corresponding author.
E-mail address: floriane.guillevic@unibas.ch (F. Guillevic).

https://doi.org/10.1016/j.jenvrad.2026.107906
Received 16 July 2025; Received in revised form 17 December 2025; Accepted 15 January 2026
Available online 28 January 2026

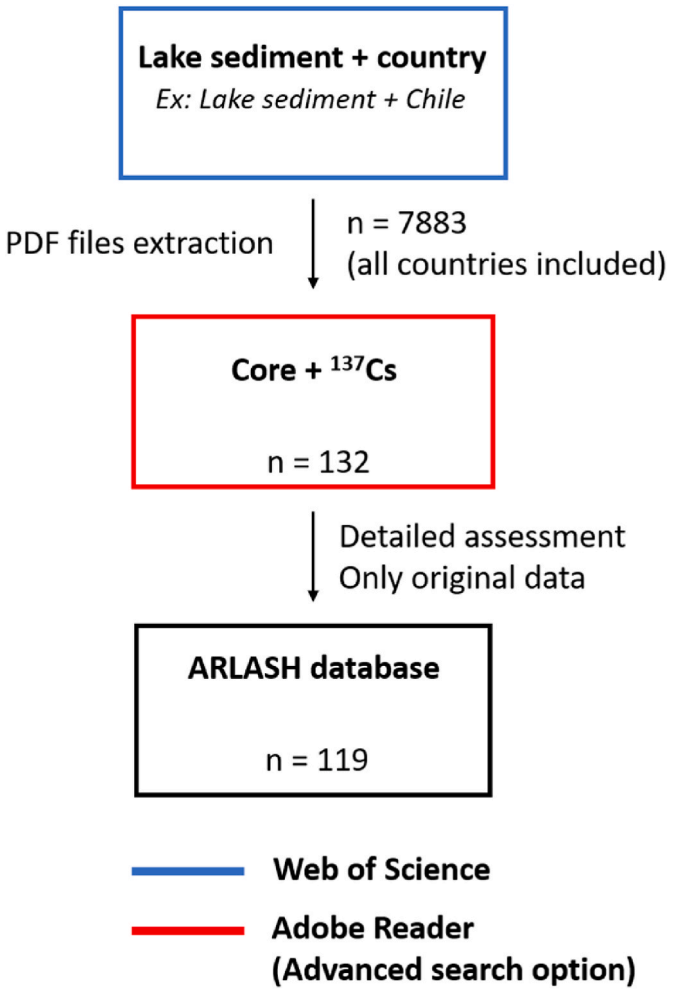

Fig. 1. Scheme of the different publication extractions from the literature review with n = total number of publication (all SH countries included).

fallout deposition in South America (Arnaud et al., 2006; Chaboche et al., 2022).

The distribution patterns of radionuclides are influenced by multiple factors, including the nature of the injection process (e.g., explosive yield, injection altitude, and latitude) and the atmospheric circulation at local, regional, and global scales (Bennett, 2002; UNSCEAR, 2000). The distribution of ^{137}Cs, which is primarily deposited through wet deposition, is significantly influenced by precipitation patterns and rates (Aoyama et al., 2006; He and Walling, 1997; Ritchie and McHenry, 1990). Moreover, the atmospheric dispersion and deposition of fallout radionuclides (FRNs) vary with proximity to nuclear test sites. Once deposited on terrestrial surfaces, the redistribution of ^{137}Cs within lake drainage areas can be influenced by factors such as vegetation and land use, lake elevation, watershed area, lake surface area, surrounding slope, and sedimentation rate, all of which affect the remobilization and deposition of FRNs in lake sediments (Appleby et al., 2019; He et al., 1996; Pulley et al., 2018; Ritchie and McHenry, 1990; Walling and Qingping, 1992).

Our knowledge of the baseline activity of ^{137}Cs in the SH is limited in comparison to that in the NH because of the limited radionuclide measurement data available in the SH (Evrard et al., 2020; Foucher et al., 2021). During the nuclear weapons testing period, the United States operated 115 monitoring stations in the NH but only 50 in the SH (Health and Safety Laboratory, 1977). While this distribution reflects the global landmass proportions (32 % in the SH vs. 68 % in the NH), the signing of the Test Ban Treaty in 1963 led to the cessation of monitoring at multiple stations around the world. This corresponds to a lack of ca. 50 % of data for the post-1963 period compared to the pre-moratorium period, with a more pronounced lack of data for the SH (Evrard et al., 2020).

Table 1
Description of the metadata in the ARLASH database extracted from the compiled literature.

Data	Variables
General information	Reservoir name, Core name, Continent, Country, Latitude, Longitude, Exact coordinates (Yes/No), Coring date, Core length, Corer type, Corer brand, Core diameter and sample depth increments
Lake information	Lake type, year of dam construction (if it is a dam lake), Lake elevation, Surface area, Maximum depth, Trophic state, Salinity
Catchment information	Surface area, Vegetation, Land use, Precipitation, Climate, Mean annual temperature
^{137}Cs data	Analysis year, Analysis technique, Activity reported (Yes/No data/DL/Reference point),^{137}Cs-based sedimentation rate, the^{137}Cs profile metrics (see paragraph 2.2) and^{137}Cs inventory
^{210}Pb data	Analysis technique, Activity reported (Yes/No data),^{210}Pb activity,^{210}Pb-based sedimentation rate, Age Model, Mass accumulation rate and^{210}Pb inventory
Sediment information	Dry bulk density, Mass depth or Cumulative dry mass
Publication information	Authors, DOI, Journal name and Publication year

In this context, a meta-analysis of lake sediment records available from the literature was conducted to identify the key factors influencing the ^{137}Cs distribution across the Southern Hemisphere. The main objectives of this study are: (i) to provide an overview of ^{137}Cs activity levels in lake sediments across continents in the SH including South America, Africa and Oceania, (ii) to compare total ^{137}Cs inventories among different lakes and (iii) to identify environmental parameters associated with spatial disparities in ^{137}Cs activity and deposition patterns.

2. Method

2.1. Data collection and ARLASH database

The literature review included all South American countries due to their proximity to Pacific nuclear weapons testing sites and the seasonal northward shift of the Intertropical Convergence Zone (ITCZ), which can extend above the Equator during the austral winter. In contrast, for Africa and Oceania, we limited our selection to countries located south of or near the equator (±1° latitude), excluding regions further north that lie predominantly within the NH.

Since ^{137}Cs is often used routinely as a time-marker radionuclide, many studies do not explicitly mention it in their titles or abstracts, which impedes the identification of these studies through standard keyword searches in literature engines. To address this, we conducted an extensive literature review covering the period from 1980 to 2024. We first used the Web of Science database to search for publications using the keywords “lake sediment” and the name of each country across the SH. In a second step, we refined the search by performing an automated keyword scan (“^{137}Cs” and “core”) within the full texts of the downloaded PDFs using Adobe Reader's advanced search function (Fig. 1).

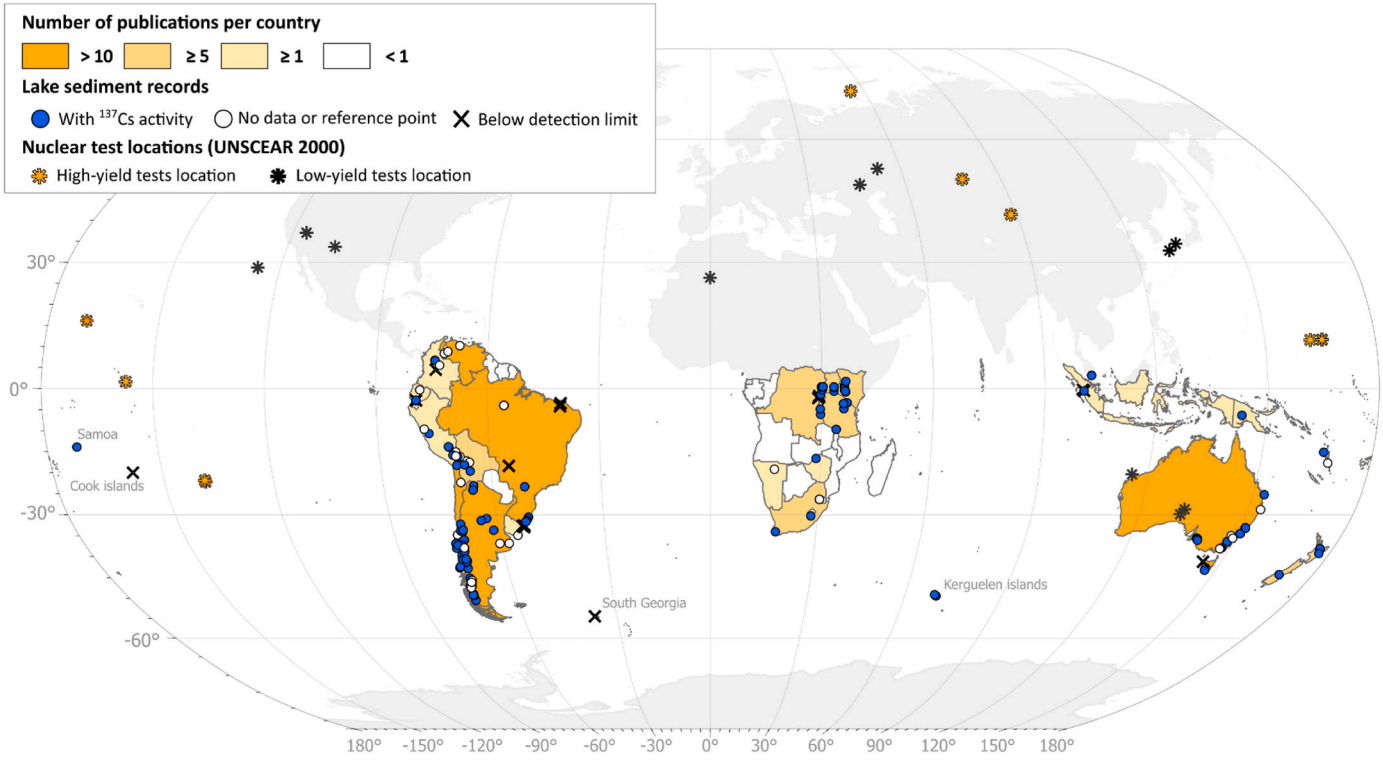

Fig. 2. Spatial distribution of lake sediment cores using ^{137}Cs activity as a time-marker in the Southern Hemisphere. Only islands with ^{137}Cs core data are labeled.

These subsearches aimed to exclude irrelevant articles, such as those that: (i) focused on suspended or surface lake sediments, (ii) lacked dating results or relied exclusively on radiocarbon (^{14}C) or optically stimulated luminescence (OSL) dating, and (iii) were unrelated to the country of interest. Peat core studies were also excluded from this review because of the higher mobility of both natural and artificial radionuclides in peat material (MacKenzie et al., 1997; Thomson et al., 2002). Accordingly, only studies assessing lakes, dams or lagoons were included.

Artificial reservoirs constructed well after the main period of fallout deposition period, or sediment cores that did not cover the pre-1960 period, were also excluded as they do not provide complete sedimentary records. Additionally, ephemeral reservoirs were excluded because of their transient hydrological nature, which likely does not lead to preserved and continuous sediment chronologies.

A careful assessment of the articles identified with the term '^{137}Cs' was conducted to retain only those with original ^{137}Cs data for the ARLASH database (**A**rtificial **R**adionuclides in **LA**ke sediments of the **S**outhern **H**emisphere). Each database entry corresponds to a sediment core in which ^{137}Cs measurements were reported. The ARLASH database is composed of sections, including general information, lake information, catchment information, ^{137}Cs data, ^{210}Pb data, sedimentation information and publication information. (Table 1). All ^{137}Cs values were decay-corrected from the year of measurement to 2025 for the meta-analysis. A more detailed description of the 55 variables extracted from the publications is available online in the metadata sheet of the ARLASH database (https://doi.org/10.5281/zenodo.15921856).

Some publications were excluded from the ^{137}Cs profile data analysis (but retained in the ARLASH database) because of certain limitations. For 33 lakes (20 % of the database), ^{137}Cs was mentioned in the methods section, but no actual data was presented in the text nor in the supplementary materials (Fig. 2, gray dots). For example, ^{137}Cs data was not provided for Laguna Blanca (Garcia-Rodriguez et al., 2002) because of the absence of a clear peak corresponding to the maximum fallout year, and for Laguna Baños (Michelutti et al., 2016) where the high organic content of the material deposited may have affected ^{137}Cs fixation and increased its mobility. For 13 lakes (8 %), only the sediment depth corresponding to the maximum fallout year (1964/1965) was referenced as a time marker, without any ^{137}Cs activity value being reported (Fig. 2, gray dots). One notable case is Lake Sibinacocha, which was included despite its chronology being based on an archaeological pot filled with sediment from the lake bottom (Michelutti et al., 2019).

Out of the 161 lakes and reservoirs from the ARLASH database, only 99 lakes (61 %) contained ^{137}Cs data presented in tables or graphs, making them suitable for further data analysis.

2.2. The ^{137}Cs total inventory

The total ^{137}Cs inventory quantifies the cumulative amount of ^{137}Cs per surface area unit, allowing comparisons across lakes irrespective of sediment density, water content or sedimentation rate. This value represents the total amount of ^{137}Cs accumulated since its first detection on global scale in 1954 CE.

Because ^{137}Cs inventories are rarely reported directly in the publications, they were calculated by interpolating the ^{137}Cs activities along the sediment core until background activity levels were reached when ^{137}Cs measurement was not continuous. The total ^{137}Cs inventory is therefore defined as the sum of the ^{137}Cs activities multiplied by the mass depth, measured continuously with a given depth interval (sampling increment):

$$Inv_{Cs} = \sum_{i=1}^{n} \left(.^{137}Cs\ activity \times DBD \times x \right) \quad \text{Equation (1)}$$

where Inv_{Cs} is in Bq.m^{-2}, the ^{137}Cs activity in Bq.kg^{-1}, the dry bulk density (DBD) in g.cm^{-3}, and x is the sampling increment thickness in cm. If available, the mass depth (g.cm^{-2}) was used directly instead of DBD multiplied by x.

When ^{137}Cs activity was not measured continuously, the data was interpolated and integrated using the *serac* R package (Bruel and Sabatier, 2020). Separate files were prepared for each lake sediment core, including DBD, ^{137}Cs activity and the top and bottom depths of

Table 2
Key metrics characterizing ^{137}Cs activity levels and their depths in sediment profiles.

	Metrics name	Description of the metric
1	**Cs_Peak64/65_Activity**	The maximum activity found in the fallout peak centred upon 1964/1965 in the SH, to capture the magnitude of the ^{137}Cs fallout from nuclear test during that specific period (in Bq.kg^{-1}).
2	**Cs_MaxActivity**	The highest activity level detected in the sediment core, which may differ from the ^{137}Cs peak associated with 1964/1965 maximum fallout and is often measured in the uppermost sediment layers of the core.
3	**Cs_AvgActivity**	The average ^{137}Cs activity of the entire core since the first detection of fallout, to summarize the overall magnitude of ^{137}Cs inputs from both fallout and catchment-derived sources (in Bq.kg^{-1}).
4	**Cs_MedActivity**	The median ^{137}Cs activity of the entire core since the first detection of fallout, to summarize the overall magnitude of ^{137}Cs inputs from both fallout and catchment-derived sources (in Bq.kg^{-1}).
5	**Cs_UpperActivity**	The activity of the uppermost sediment layer (0–2 cm) expressed as a percentage of the maximum activity measured in the core, to analyse recent inputs of ^{137}Cs in comparison with those from the peak fallout period (in Bq.kg^{-1}).
6	**Cs_IncreaseDepth**	Depth of the beginning of the 1964/1965 peak (in cm).
7	**Cs_DecreaseDepth**	Depth of the end of the peak (in cm).
8	**Cs_AboveDL_Depth**	Depth of the 1st occurrence of ^{137}Cs activity above detection limit which represents the deepest sediment layer where ^{137}Cs is measurable or reported (in cm).
9	**Cs_Peak64/65_Depth**	Depth of the maximum activity found in the fallout peak (in cm).
10	**Cs_MaxDepth**	Depth of the maximum ^{137}Cs value if different than Cs_Peak64/65Depth (in cm).

Table 3
Description of the environmental variables extracted for each lake.

	Variable name	Description of the variable	Source/Method
1	Lake_Area	Surface area of the lake (in km^2)	HydroLAKES database[a] (Messager et al., 2016)
2	Catch_Area	Area of the lake's contributing catchment (in km^2)	HydroLAKES database[a] (Messager et al., 2016)
3	Ratio_CL	Ratio of catchment area to lake surface area	
4	Precipitation_WorldClim	Long-term mean annual precipitation (1950–2000, in mm)	Worldclim v1.4 database (Hijmans et al., 2005)
5	NEAR_dist_MR	Euclidean distance from Mururoa from each lake to the Mururoa test site (in km)	Calculated using ArcGIS
6	FALSE_dist_MR	Westward component of distance to Mururoa, to reflect prevailing wind direction Westward distance from Mururoa (in km)	Calculated using ArcGIS
7	LAT_DEC	Latitude used as a proxy for distance from the equator and, by extension, from the Northern Hemisphere, where most nuclear tests occurred (in decimal degree)	Reported by the authors or determined from maps and satellite images
8	Lake_elev	Elevation of the lake (in m)	Reported by the authors
9	Lake_depth	Maximum lake depth (in m)	Reported by the authors

[a] for lakes larger than 0.1 km^2.

each sample to compute the ^{137}Cs total inventory. To enable comparisons across lakes, all ^{137}Cs activities and inventories were decay-corrected to the year 2025 using the following equation:

$$Inv_{Cs\_2025} = Inv_{Cs} * e^{-\frac{\ln 2}{\tau_{1/2}} * t} \quad \text{Equation (2)}$$

Where t = 2025-Year of measurement and $\tau_{1/2}$ is the half-life of ^{137}Cs (30.2 years).

We assume that ^{137}Cs measurements were conducted one year after core collection unless otherwise specified. When not specified, the core collection year was estimated based on an average five-year gap observed between collection and publication dates in the database. A similar time lag has also been reported for ^{137}Cs inventories from reference soil profiles studies (Dicen et al., 2025; Jagercikova et al., 2015).

2.3. The ^{137}Cs profile metrics

A comparison of the ^{137}Cs profile was conducted using data extracted from tables and graphs in publications included in the ARLASH database. For each core, ten descriptive metrics were compiled to characterize the magnitude and depth distribution of ^{137}Cs in sediment cores, including different activity levels at key period depth markers (Table 2).

When numerical data tables were unavailable, depth and activity values were digitized from ^{137}Cs profile plots using WebPlotDigitizer (Rohatgi, 2015).Of the 134 records (from 99 lakes), only 15 % provided data in table format and were directly useable, while the remaining 85 % were digitized from figures.

To identify patterns and classify profiles following their shape, a principal component analysis (PCA) followed by hierarchical clustering was conducted using the FactoMineR package in R (Lê et al., 2008; R Core Team, 2024).This multivariate approach aims to reduce the number of variables and identify groupings among profiles based on the variations in ^{137}Cs metrics. Missing values were imputed using the mean of each variable using the imputePCA function from the missMDA package (Josse and Husson, 2016).

2.4. Relationships between environmental parameters and ^{137}Cs activity

To evaluate the influence of the environmental settings on the distribution of ^{137}Cs in lake sediments across the SH, we tested the relationships between a set of eight climatic and geographic variables and ^{137}Cs activity metrics.

When environmental data was not reported by the authors, we extracted the lake surface area and catchment size from the HydroLAKES database (Messager et al., 2016) and the mean annual precipitation from the WorldClim v1.4 database (Hijmans et al., 2005) using ArcGIS Pro 3.0.3 (Table 3). In addition, we calculated the Euclidean distance and the westward distance to the Mururoa and Fangataufa nuclear test sites, to account for both geographic proximity and prevailing wind patterns that may have influenced the fallout distribution.

The environmental parameters were first compared with the ^{137}Cs peak activity alone, and then with the ratio of the ^{137}Cs peak activity to the sedimentation rate (i.e., the peak activity normalized by the sedimentation rate). This ratio was introduced to account for potential sediment dilution effects and to improve comparability between lakes with different sediment accumulation dynamics.

We applied a range of statistical techniques using R v.4.3.3 (R Core Team, 2024), including Spearman's rank correlation to assess relationships between individual variables, multiple linear regression to evaluate the combined influence of potential predictors, and random forest analysis to identify the most influential variables. Differences in the

environmental parameters across the ^{137}Cs profile groups (as defined by PCA-based clustering) were assessed using the Kruskal-Wallis test. This suite of methods allowed us to explore both continuous trends and group-level contrasts in the environmental drivers of ^{137}Cs deposition in lake sediments.

3. Results and discussion

3.1. Lake distribution of the ARLASH database

3.1.1. Data spatial distribution

Using the search term "lake sediment" combined with the name of each country, we extracted over 8000 research publications published from 1980 to 2024 from the Web of Science (Clarivate Analytics) database. A detailed review was conducted on all publications that included ^{137}Cs data (2 % of the initial search). After excluding citation-based papers and retaining only original published data, 119 publications in which ^{137}Cs was measured were included in the ARLASH database (Fig. 1). Notably, 95 % of these publications (n = 114, where n refers to the number of publications) also reported ^{210}Pb data.

This two-step literature review allowed us to study multiple publications dealing with lake sediment dating using ^{137}Cs as the only recent time marker or used in combination with excess ^{210}Pb. A previous literature review conducted by Foucher et al. (2021), which used the search terms "^{137}Cs" and "sediment core", identified 27 lakes in the SH (including lagoons and dam reservoirs) from 19 publications out of a total of 1300 sediment records globally, mainly originating from marine coastal and estuarine environments. Our approach yielded five times more studies, substantially improving the spatial coverage of ^{137}Cs-based lake sediment chronologies in the SH.

However, the number of lakes with ^{137}Cs data in the SH corresponds to less than half the number reported for the Northern Hemisphere (Foucher et al., 2021).This gap would likely increase if the two-step literature review was applied to the Northern Hemisphere, where glacial and periglacial processes contribute to a greater number of lakes.

Each record in the ARLASH database corresponds to a sediment core with reported ^{137}Cs measurements (202 cores). Typically, one core per lake was analysed, although in 15 % of the cases, multiple cores were obtained from the same lake. In total, 161 lakes from the Southern Hemisphere were included: 94 lakes from South America, 35 lakes from Africa, 29 lakes from Oceania (including Melanesia and Micronesia) and 3 lakes from Southeast Asia. The geographical distribution of studies is heterogeneous, with South America accounting for the largest proportion (58 %), followed by Africa (22 %) and Oceania (18 %). The majority of studies were conducted in Chile and Argentina, followed by Australia and Uganda (Fig. 2).

The spatial distribution of study sites using ^{137}Cs as an independent time marker to date lake sediment cores mirrors the distribution of permanent freshwater lakes in the SH. Africa shows particularly an uneven distribution, with most ^{137}Cs-based studies concentrated in the African Great Lakes region and the Rwenzori Mountains (0–10°S). This pattern reflects the concentration of large tropical open freshwater lakes in the western branch of the East African Rift, which are less sensitive to hydroclimatic changes (Branchu et al., 2010), as well as the limited number of permanent freshwater lakes in southern Africa (below 17°S latitude) suitable for preserving continuous sediment records (Rose et al., 2021). However, Rose et al. (2021) identified several lakes in Mozambique that are promising for reconstructing recent anthropogenic impacts, although no ^{137}Cs study has been conducted in this region so far (Fig. 2).

In South America, most studies are restricted to the Andes Mountains or their foothills (Fig. 2), particularly in the lake district and its myriad of glacial lakes that extend across Chile and Argentina (38–43°S) where glacial lakes offer favorable settings for preserving sediment sequences. In contrast, no ^{137}Cs-based published data has been found in countries such as Paraguay, Suriname and Guyana, or the overseas department of French Guiana. In addition, lowland agricultural regions such as the Pampa of Argentina, Uruguay and Southern Brazil are underrepresented in ^{137}Cs studies. These areas have undergone massive land use changes over recent decades, which have increased erosion and subsequently increased sediment input as well as contaminants transfers such as pesticides to lacustrine systems (Foucher et al., 2023). More studies could likely use ^{137}Cs to reconstruct recent environmental changes in these areas.

In Oceania, most of the publications are concentrated along Australia's eastern coast (Fig. 2). Generally, there is a notable scarcity of ^{137}Cs data across much of the 20–30°S latitudinal band in the SH.

3.1.2. Factors limiting the detection of ^{137}Cs activity peak

The detection of the ^{137}Cs activity peak in the Southern Hemisphere is known to be limited by the low artificial fallout deposition, which is approximately three times lower than in the Northern Hemisphere, as most nuclear weapons tests were conducted there (UNSEAR 1982). This section reports on the main challenges encountered when measuring ^{137}Cs activity.

The ^{137}Cs activity was reported to be below the detection limits in 16 lakes (10 % of records, Fig. 2). The only reported detection limit for these publications is the one given by Godoy et al. (2002) equal to 3 Bq.kg^{-1}. The reported detection limits in the other cases typically range from 1 to 2 Bq.kg^{-1} (Arnaud et al. 2016: 2 Bq.kg^{-1}; Daga et al., 2008: 1 Bq.kg^{-1}; Guilizzoni et al., 2009: 1 Bq.kg^{-1}; Ribeiro Guevarra and Arribere, 2002: 1 Bq.kg^{-1} and Wils et al., 2021: 1 Bq.kg^{-1}). Although these detection limits are not particularly high, elevated detection limits (>1 Bq.kg^{-1}) may in some cases mask the occurrence of low although significant ^{137}Cs activity, particularly in the SH.

Low ^{137}Cs activities associated with high uncertainties were reported for Laguna Fondacocha and Llaviucu (Ecuador) with values of 5.6 ± 3.0 Bq.kg^{-1} and 2.5 ± 1.1 Bq.kg^{-1} respectively, (Bandowe et al., 2018), complicating the identification of the ^{137}Cs peak. In the future, this issue may be addressed using ultra-low background ^{137}Cs measurement facilities, such as those available in underground laboratories (Reyss et al., 1995).

Low annual rainfall at the lake location is another cited factor associated with low or the absence of detection of ^{137}Cs, as observed in arid to semi-arid regions such as Lago Vichuquén in Central Chile (Frugone-Alvarez et al., 2017) or the Acaraú-Mirim and Araras dams in northeast semi-arid part of Brazil (Ledru et al., 2020).

Sediment mixing can result from the input of material derived from erosion processes, turbidite deposition, flooding events, or bioturbation. These processes can redistribute ^{137}Cs within the sediment core, thereby causing lower activity levels that may obscure the ^{137}Cs activity peak. For instance, the Acaraú-Mirim and Araras reservoirs (Brazil) showed no detectable ^{137}Cs, likely because of high sediment inputs following their recent construction years (1961 and 1958 respectively, Ledru et al., 2020). Shallow coastal freshwater lakes such as the Mangueira and Mirim lagoons and Lake Nicola (Brazil) also showed no ^{137}Cs, likely because of sediment resuspension in shallow basins (<5m, Bueno et al., 2021). Conversely, in Lake Titicaca (Peru/Bolivia), a very low sedimentation rate combined with a too thick sampling resolution likely resulted in temporal averaging of ^{137}Cs concentrations, smoothing out the ^{137}Cs activity peak and complicating its detection (Guédron et al., 2021). A similar challenge was reported for Lake Nahuel Huapi, where low sedimentation rate combined with 2 cm sub-sampling resolution prevented the distinction of ^{137}Cs fallout peaks in the activity profiles (Ribeiro Guevara and Arribére, 2002). A discontinuous sampling strategy can likewise lead to miss the ^{137}Cs peak (e.g., Lake Rotorua, New Zealand, Weisbrod et al., 2020).

Non-ideal coring locations may also result in undetectable ^{137}Cs peaks. In Lake Kivu (Rwanda), coring was conducted along the lake shore to avoid high gas concentrations found below 200 m in depth, potentially leading to the loss of surface sediment (Pasche et al., 2010). In contrast, in Lakes Singkarak and Maninjau (Indonesia), the absence of

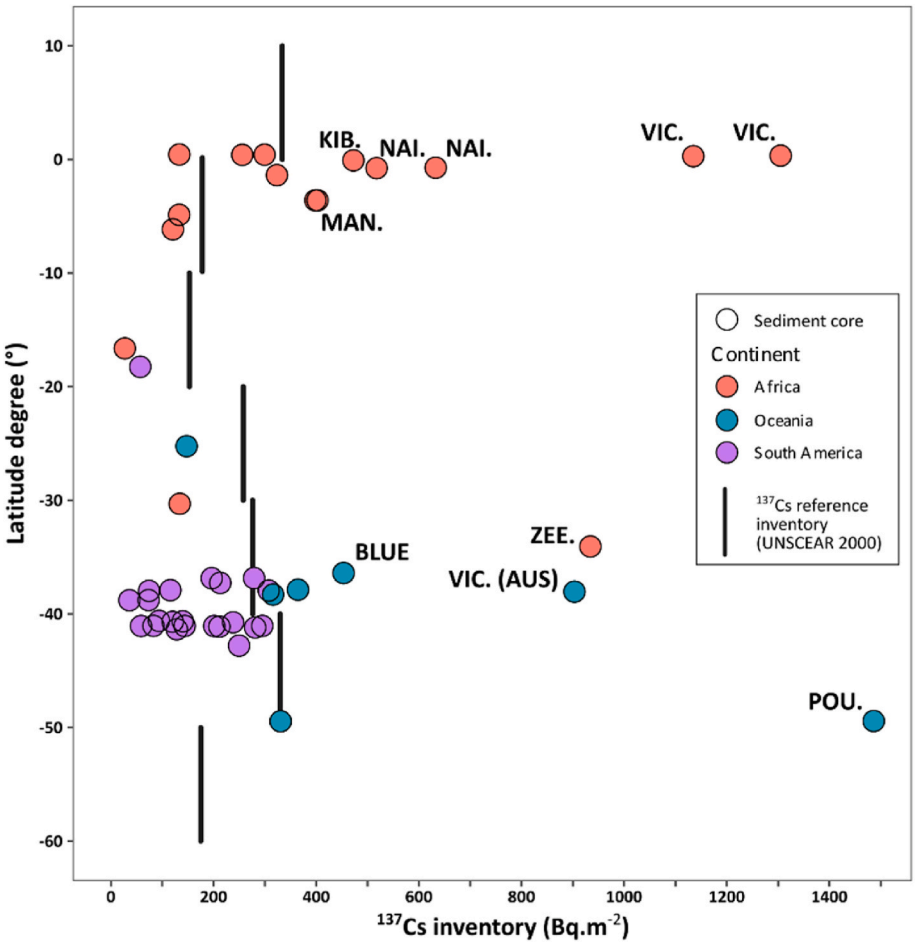

Fig. 3. Latitude versus ^{137}Cs inventories derived from ARLASH data publications and from atmospheric latitudinal deposition (UNSCEAR, 2000). Lakes with inventories higher than 400 Bq.m^{-2}are Lake Victoria (VIC.), Lake Zeekoevlei (ZEE.), Lake Kibengo (KIB.), Lake Manyara (MAN.), Lake Victoria in Australia (VIC. AUS), Lake Blue (BLUE), Lac de la Poule (POU.). The ^{137}Cs inventories were decay corrected to 2025. (For interpretation of the references to color in this figure legend, the reader is referred to the Web version of this article.)

^{137}Cs may be attributed to high sedimentation rates at deep coring sites, potentially enhanced by sediment focusing, which dilutes the ^{137}Cs activity (Wils et al., 2021). Sediment focusing refers to the lateral redistribution of sediments within a lake basin which leads to enhanced accumulation in deeper areas compared to shallower zones (Corcoran et al., 2018; Edgington and Robbins, 1990). In some cases, no specific explanation was provided for such an absence of detection: Laguna de Ubaque (Colombia, Bird et al., 2018), Lake Fan (South Georgia, Strother et al., 2015) or Rebecca Lagoon (Tasmania, Saunders et al., 2012).

The publications included in the database did not directly address the influence of organic matter content and particle size distribution on the detection and distribution of ^{137}Cs in lake sediments. However, these factors are known to affect these processes. Typically, ^{137}Cs activities are higher in fine-grained sediments and show a strong affinity for organic matter (Pulley et al., 2018).

Overall, the detection of ^{137}Cs activity in the Southern Hemisphere is limited by low fallout deposition and spatial variability in precipitation, with additional limitations arising from variable sedimentation dynamics (e.g., high versus low sedimentation rate) and sampling strategies (e.g., sampling resolution, coring site).

Another key factor that can limit the use of ^{137}Cs to validate recent chronologies is the lack of access to measurement infrastructures. There is no record of any African laboratory measuring natural or artificial radionuclides in the ARLASH database. In South America, only a few laboratories are mentioned, one in Argentina and another in Chile. Many researchers send samples to the NH (e.g., to labs in the U.S., Canada, France, or the UK) where low-background Germanium detectors are generally used for radionuclide measurements, which limit regional capacities in obtaining recent sediment chronology and the development of studies focused on recent environmental changes that require sediment dating as a prerequisite.

3.2. Total ^{137}Cs inventories

Dry bulk density or cumulative mass depth data were provided for only 23 % of the sediment cores, allowing the calculation of ^{137}Cs inventories for 45 cores collected in 29 lakes across the SH. The median ^{137}Cs inventory across these sites is 239 Bq.m^{-2} (IQR: 129–365 Bq.m^{-2}; Min-Max: 27–1488 Bq.m^{-2}). On average, the lake sediment ^{137}Cs inventories are consistent with the reference fallout values reported by UNSCEAR (2000), which range from 200 Bq.m^{-2} near the equator to 400 Bq.m^{-2} between 40° and 50°S latitude (Fig. 3). Continental median inventories were calculated as follows: 142 Bq.m^{-2} for South America (22 cores; IQR: 86–232 Bq.m^{-2}), 361 Bq.m^{-2} for Africa (16 cores; IQR: 134–547 Bq.m^{-2}) and 365 Bq.m^{-2} for Oceania (7 cores; IQR: 324–680 Bq.m^{-2}). Only a small number of lakes in the ARLASH database show ^{137}Cs inventories exceeding 400 Bq.m^{-2}:

- Lac de la Poule (Kerguelen Islands, 1488 Bq.m^{-2}),
- Lake Victoria (Uganda, 1309 and 1138 Bq.m^{-2}),
- Lake Zeekoevlei (South Africa, 936 Bq.m^{-2}),
- Lake Victoria (Australia, 905 Bq.m^{-2}),

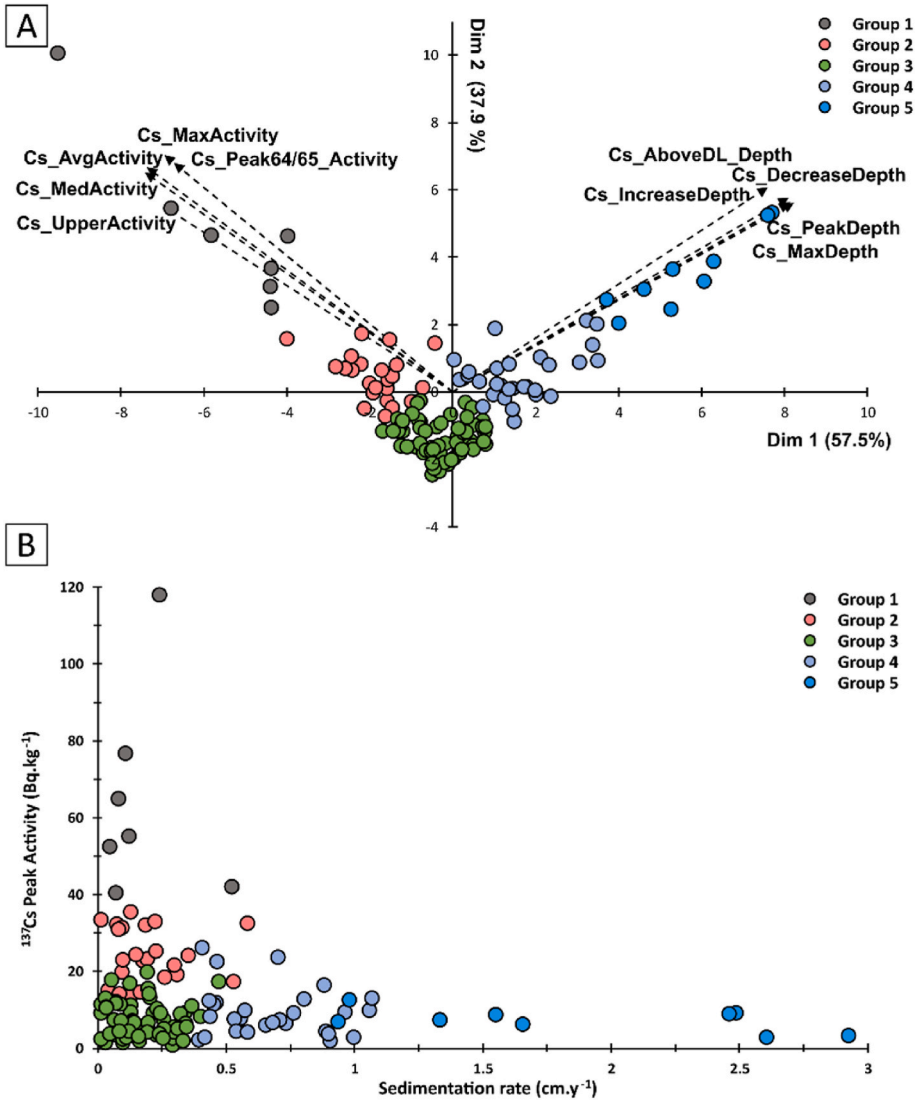

Fig. 4. A - Principal component analysis of the ^{137}Cs metrics used to characterize each ^{137}Cs profile with groups determined using hierarchical cluster analysis. B- Simplification of the lake sediment core classification based on the ^{137}Cs peak activity (Bq.kg-1) and the ^{137}Cs-based sedimentation rate (cm.yr^{-1}).

- Lake Naivasha (Kenya, 633 and 518 Bq.m^{-2}),
- Lake Kibengo (Uganda, 474 Bq.m^{-2}),
- Blue Lake (Australia, 455 Bq.m^{-2})
- Lake Manyara (Tanzania, 403 and 399 Bq.m^{-2}).

Large lakes such as Lake Victoria and Lake Naivasha in the Rift Valley (Africa) have extensive surface areas and drain large basins, which promote significant sediment remobilization across the catchment. This process can lead to sediment focusing from shallow to deeper areas, resulting in elevated ^{137}Cs inventories, and could explain why a third sediment core from Lake Victoria (core NG1) shows a much lower ^{137}Cs inventory of 255 Bq·m^{-2} (Stager et al., 2009). In Africa, most lake sediment inventories are available for equatorial regions, where ^{137}Cs fallout has been reported to be higher compared to other parts of the SH (UNSCEAR, 2000).

Lake Victoria in Australia, one of the country's largest freshwater lakes, also exhibits high ^{137}Cs accumulation, which is likely driven by watershed-derived inputs and sediment focusing. Similarly, the Lake de la Poule in the Kerguelen Islands stands out with a high inventory, possibly reflecting unique regional deposition patterns and sediment dynamics, with very recent erosion from the catchment (Ficetola et al., 2018). Overall, lakes with larger catchments and more dynamic sediment processes tend to accumulate more ^{137}Cs-labeled material from the watershed.

In South America, most lakes with reported ^{137}Cs inventories are located between 35° and 45°S latitude. These sites generally show inventories consistent with, or slightly below, UNSCEAR reference values and are typically small, high-altitude lakes with limited catchment areas.

Due to the limited number of publications providing dry bulk density (DBD) or cumulative mass depth data, it remains challenging to compare ^{137}Cs deposition quantitatively across the SH using lake inventories. In contrast, ^{137}Cs metrics such as activity levels and depth profiles are more consistently available and are often more suitable for inter-lake comparisons.

SH lake inventories are roughly an order of magnitude lower than those found in the Northern Hemisphere, where the median ^{137}Cs inventory for lacustrine environments is 1316 Bq.m^{-2} (n = 216, Foucher et al., 2021). In South America, computed inventories are primarily concentrated between 35 and 45°S latitude, aligning with the expected latitudinal range of ^{137}Cs deposition (Fig. 3). However, potential intercontinental differences are not accounted in the UNSCEAR reference inventory estimates (UNSCEAR, 2000). The total ^{137}Cs inventories across the SH are variable, with higher values in equatorial Africa and

Table 4
Basic statistics per lake group defined by hierarchical clustering.

		^{137}Cs maximum activity peak (Bq.kg^{-1})			^{137}Cs median activity (Bq.kg^{-1})			Depth of ^{137}Cs activity peak (cm)			^{137}Cs sedimentation rate (cm.yr^{-1})		
		Min	*Max*	*Median*	*Min*	*Max*	*Median*	*Min*	*Max*	*Median*	*Min*	*Max*	*Median*
Group 1	(max n = 7)	40.5	118.1	**55.3**	27.2	71.7	**33.3**	1.0	21.0	4.5	0.05	0.53	0.11
Group 2	(max n = 23)	14.1	35.5	**23.4**	9.2	26.0	**14.0**	0.8	21.0	6.25	0.01	0.58	0.17
Group 3	(max n = 66)	0.9	19.8	6.2	0.3	10.8	3.4	0.5	17.0	6.75	0.01	0.47	0.16
Group 4	(max n = 29)	2.1	26.3	7.8	0.4	12.7	4.0	18.0	52.0	**27.5**	0.39	1.07	**0.65**
Group 5	(max n = 9)	2.8	12.5	7.4	0.4	6.8	2.5	46.0	97.0	**72**	0.94	2.93	**1.66**

lower values in South America and Oceania. These patterns are likely influenced by the combination of fallout distribution, catchment characteristics, and sedimentation dynamics. The overall lower inventories in the SH relative to those of the Northern Hemisphere are consistent with established global fallout patterns (UNSCEAR, 2000; Foucher et al., 2021). Although the limited number of computed inventories in the ARLASH database prevents robust latitudinal comparisons, some equatorial African lakes show high ^{137}Cs inventories. This pattern aligns with reference soil inventories compiled by Dicen et al. (2025), which report the highest values between 0 and 10° latitude in Africa, reflecting the influence of NH fallout.

3.3. A comparative analysis of ^{137}Cs sediment profiles

The maximum ^{137}Cs activity in each sediment core is generally interpreted by the authors in the SH as corresponding to the global fallout peak in 1964/1965 and can be representative of the magnitude of ^{137}Cs deposition at each site. Across 99 lakes, the median ^{137}Cs peak activity is 7.3 Bq·kg^{-1} (decay-corrected to 2025, IQR: 3.4–14.2 Bq.kg^{-1}), with values ranging from 0.27 to a maximum of 118 Bq·kg^{-1}

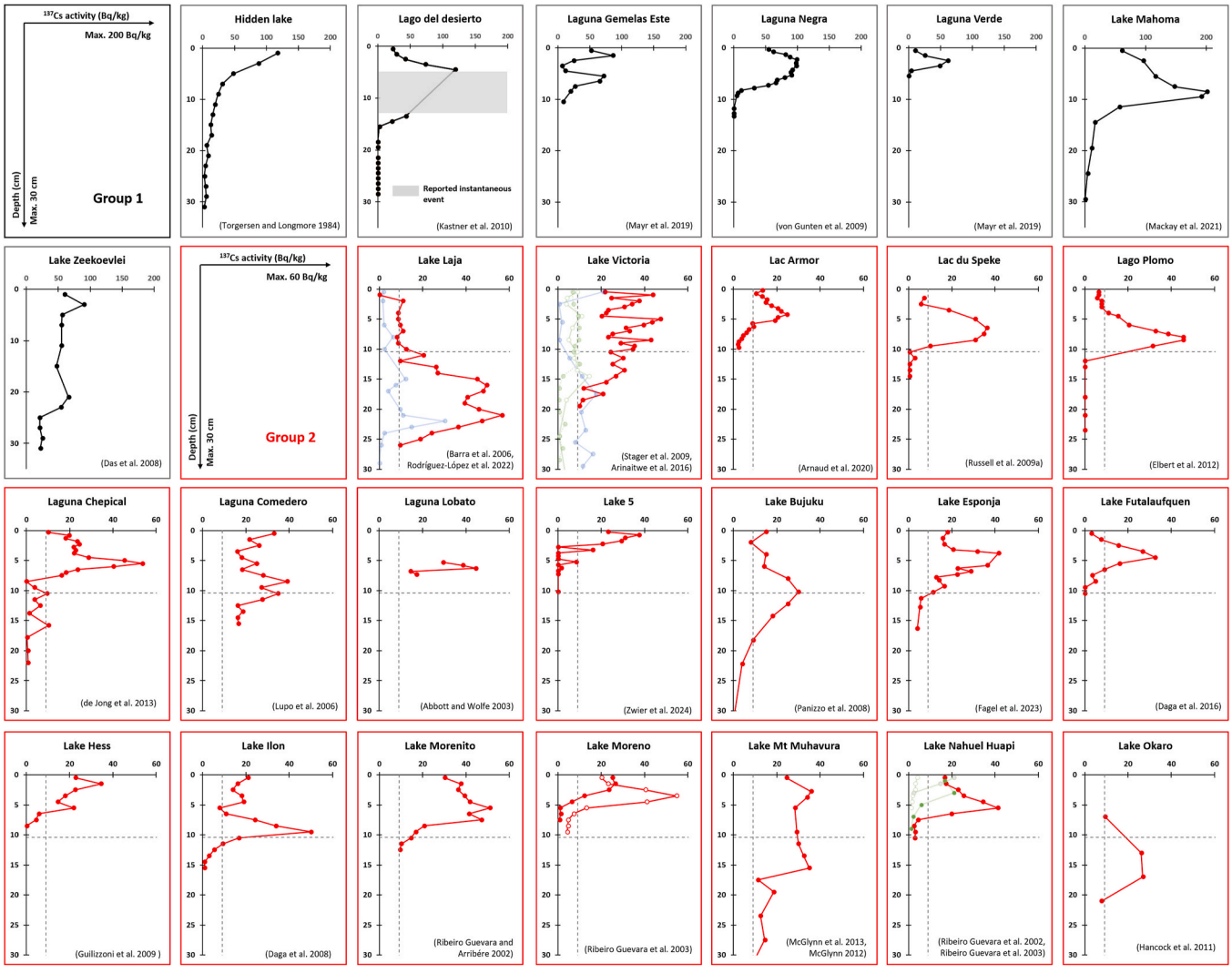

Fig. 5. Profiles of the five groups identified during clustering: Group 1 (high ^{137}Cs - low sedimentation rate), Group 2 (intermediate ^{137}Cs – low sedimentation rate), Group 3 (low ^{137}Cs – low sedimentation rate), Group 4 (low ^{137}Cs – high sedimentation rate) and Group 5 (low ^{137}Cs – high sedimentation. The vertical and horizontal gray dotted lines represent the average depth and activity of the ^{137}Cs activity peak. All references to this figure are listed in the ARLASH database. Different Transparent colors for a graph indicate cores from the same lake but in different groups. (For interpretation of the references to color in this figure legend, the reader is referred to the Web version of this article.)

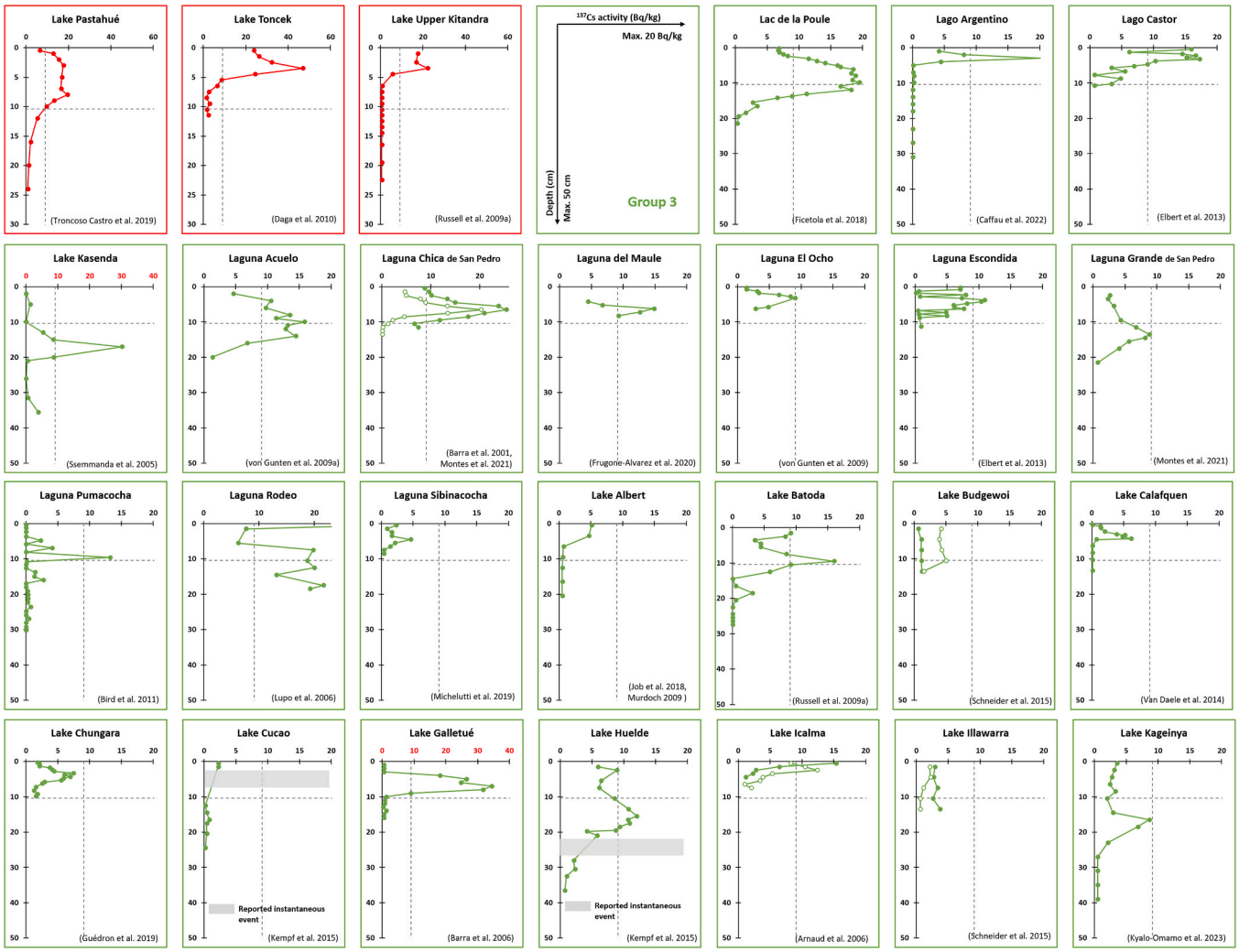

Fig. 5. (*continued*).

recorded in Lake Mahoma (Uganda; Mackay et al., 2021). Median peak activities by continent vary as follows: 9.1 Bq·kg^{-1} in South America (IQR:4.1–18.1 Bq.kg^{-1}), 8.6 Bq·kg^{-1} in Africa (IQR:5.0–13.0 Bq.kg^{-1}), 4.8 Bq·kg^{-1} in Oceania (IQR: 2.8–9.3 Bq.kg^{-1}), and 2.8 Bq·kg^{-1} in Asia (IQR: 0.4–2.8 Bq.kg^{-1}).

These peaks are seven to fourteen times in average lower than those reported by Foucher et al. (2021) in NH lakes (69.8 ± 91 Bq.kg^{-1}). This discrepancy is attributed primarily to the greater distance of the SH from the main nuclear weapons testing sites, most of which were located in the Northern Hemisphere. As noted by UNSCEAR (2000), only about 30 % of global artificial radionuclide fallout occurred in the SH, resulting in lower initial deposition levels of ^{137}Cs.

The low ^{137}Cs activity in SH lake sediments reinforces concerns about the future detectability and use of this artificial radionuclide for dating archives. Continuous radioactive decay will further reduce ^{137}Cs activities, and within a few decades, many profiles may fall below analytical detection. Based on decay projections, after two half-lives of ^{137}Cs (~60 years), approximately 64 % of the lake records in the ARLASH database would have peak activities below 3 Bq·kg^{-1} which poses significant challenges for their use as reliable chronological markers. To better understand the variability of the ^{137}Cs profiles, we applied clustering methods to group lakes with similar ^{137}Cs profiles and metrics, which most likely are linked to differences in sedimentation dynamics.

Clustering analysis of ^{137}Cs profiles

Hierarchical Clustering on Principal Components (HCPC) was used to classify ^{137}Cs sediment profiles, based on the ^{137}Cs activities and depth metrics (Table 2). The first principal dimension (dim 1 = 57.5 %) captures most of the total variance in the database and corresponds to positive loading variation in depth-related metrics, including the depth of the ^{137}Cs peak, maximum depth, and depth range over the ^{137}Cs activity peak (Fig. 4A). Positive loading on this axis captures variability in the sediment accumulation. Negative loading on dim 1 is more strongly associated with ^{137}Cs activity metrics such as peak, average, and maximum activity. This negative loading on dim 1 reflects the magnitude of ^{137}Cs deposition across profiles. The second principal dimension (dim 2 = 37.9 %) allows only to separate the Group 3 lakes to the rest of the groups with a positive loading on dim 2. The third principal dimension only accounts for less than 3 % of the variance in the dataset (Fig. S1).

The first dimension highlights a gradient from profiles with low activity and deep ^{137}Cs activity peaks (positive loading of Dim 1) to those with high activity peaks near the sediment surface (negative loading of Dim 1) illustrating the influence of the sedimentation rate on the magnitude of ^{137}Cs activity. Based on cluster inertia gain lower than 1, five distinct groups were defined (Fig. S2, Fig. 4A). Each group represents different ^{137}Cs activity profiles varying in ^{137}Cs activity levels, and depth characteristics (Table 4).

To simplify group interpretation, we summarized ^{137}Cs profile

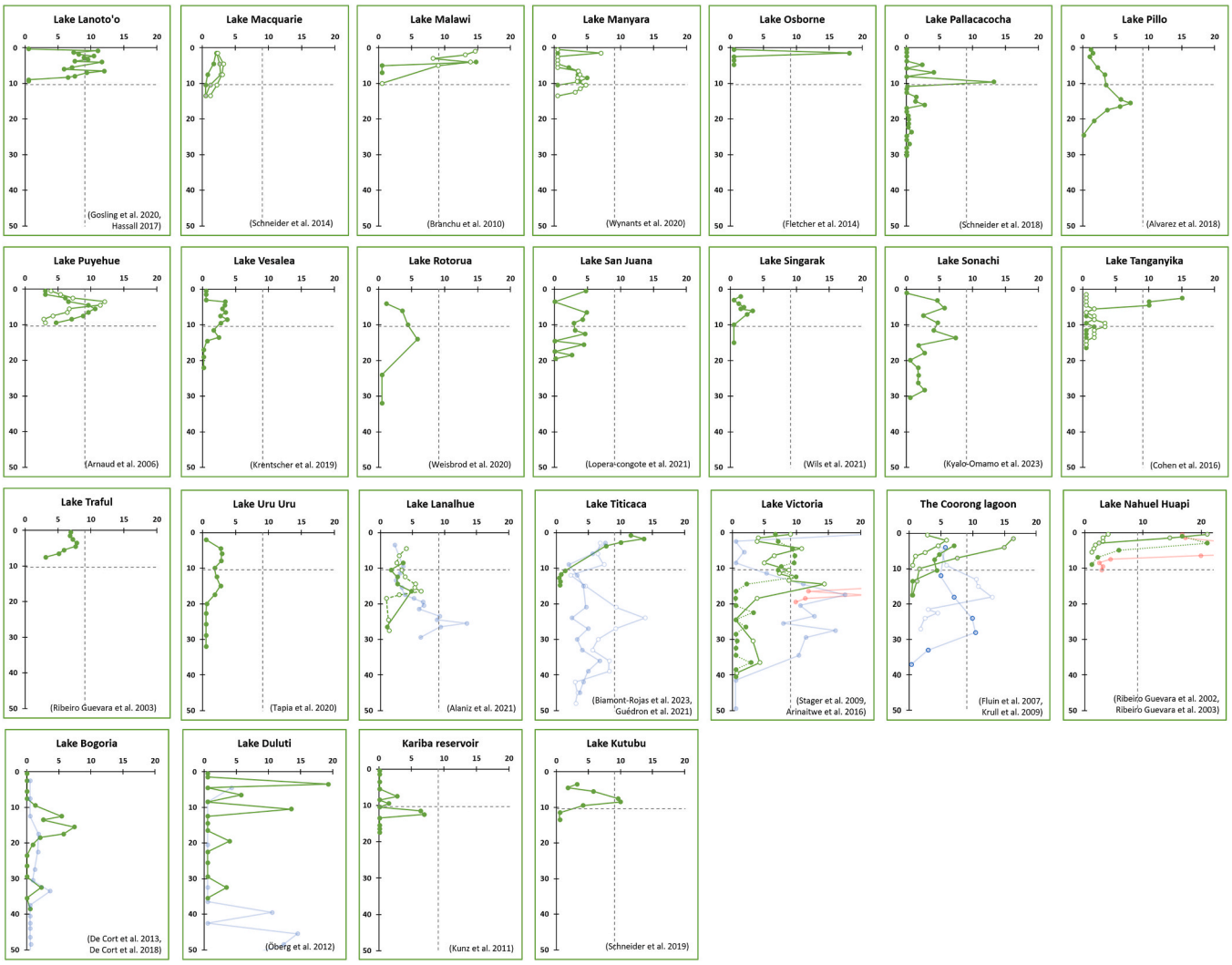

Fig. 5. (*continued*).

metrics variability with the ^{137}Cs activity peak, and the sedimentation rate was estimated by dividing the depth of the ^{137}Cs activity peak (assumed to correspond to the 1964/1965 fallout maximum) by the time since coring (Fig. 4B). The sedimentation rates were estimated based on ^{137}Cs because $^{210}Pb_{ex}$-derived rates were sometimes unavailable or reported only as ranges throughout the core. This calculated sedimentation rate provides a straightforward metric to describe sediment accumulation dynamics across lakes. The different lake groups were plotted on a map (Fig. S3) to better visualize their spatial distributions and to identify potential hotspots of ^{137}Cs deposition.

Group 1 – Very high ^{137}Cs activity peak with low sedimentation rates

Lakes in Group 1 (n = 7) are characterized by a high median ^{137}Cs activity peak of 55.4 Bq.kg-^{1} (IQR:47.3–71.1 Bq.kg^{-1}) associated with a shallow peak depth, which represents a low median sedimentation rate of 0.11 cm.yr^{-1} (IQR:0.08–0.18, Table 4). This group is very distinctive from the other four groups with a^{137}Cs maximum activity peak five times higher than the median maximum ^{137}Cs activity peak (Fig. 4B). This group includes only seven lakes: Lago del Desierto, Laguna Gemelas Este and Laguna Verde (Argentina), Laguna Negra (Chile), Lake Zeekoevlei (South Africa), and Lake Mahoma (Uganda). Lake Zeekoevlei is the only lake from group 1 that shows a mixed ^{137}Cs profile without a clear ^{137}Cs peak (Fig. 5). Most of these lakes are located between 30 and 50° S latitude, except for Lake Mahoma, which is located at the equator (Fig. S3).

Group 2– Intermediate ^{137}Cs activity peak group with low sedimentation rates

Lakes in Group 2 (n = 23) present low sedimentation rates (median: 0.17 cm.yr^{-1}; IQR:0.10–0.25 cm.yr^{-1}), comparable to those in Group 1, but with the ^{137}Cs peak activity being approximately half as high (median: 23.5 Bq.kg^{-1}; IQR: 18.8–31.9 Bq.kg^{-1}, Table 4). These lakes are located primarily between 30 and 50° S latitude in South America and in the Rwenzori Mountains at the equator in Africa (Fig. S3). The relatively high ^{137}Cs levels observed in some equatorial lakes may be attributed to additional fallout from the Northern Hemisphere.

Group 3 – Low ^{137}Cs activity peak with low sedimentation rates

Lakes in Group 3 (n = 66) represent the largest cluster in the dataset and are characterized also by low sedimentation rates (0.16 cm yr^{-1}; 0.09–0.26 cm.yr^{-1}), similar to those of Groups 1 and 2. However, the ^{137}Cs activity peak in these lakes was relatively low (6.2 Bq·kg^{-1}; 3.9–10.1 Bq.kg^{-1}, Table 4), falling below the overall median value. These lakes are distributed mainly between 25° and 50°S in South America, with six additional lakes located near the equator in Africa (Fig. S3). While Groups 1 and 2 include only a few lakes in Africa and Oceania, Group 3 is the most representative in these two regions. Compared with the clear ^{137}Cs peaks observed in Groups 1 and 2, the peak in Group 3 lakes is often less distinct or even absent (Fig. 5).

Group 4– Low ^{137}Cs peak activity with high sedimentation rates

Lakes in Group 4 (n = 29) present a low ^{137}Cs activity peak (7.9 Bq. kg^{-1}; 4.4–11.9 Bq.kg^{-1}), similar to those in Group 3, but were characterized by a relatively high sedimentation rate (0.65 cm.yr^{-1}; 0.47–0.88

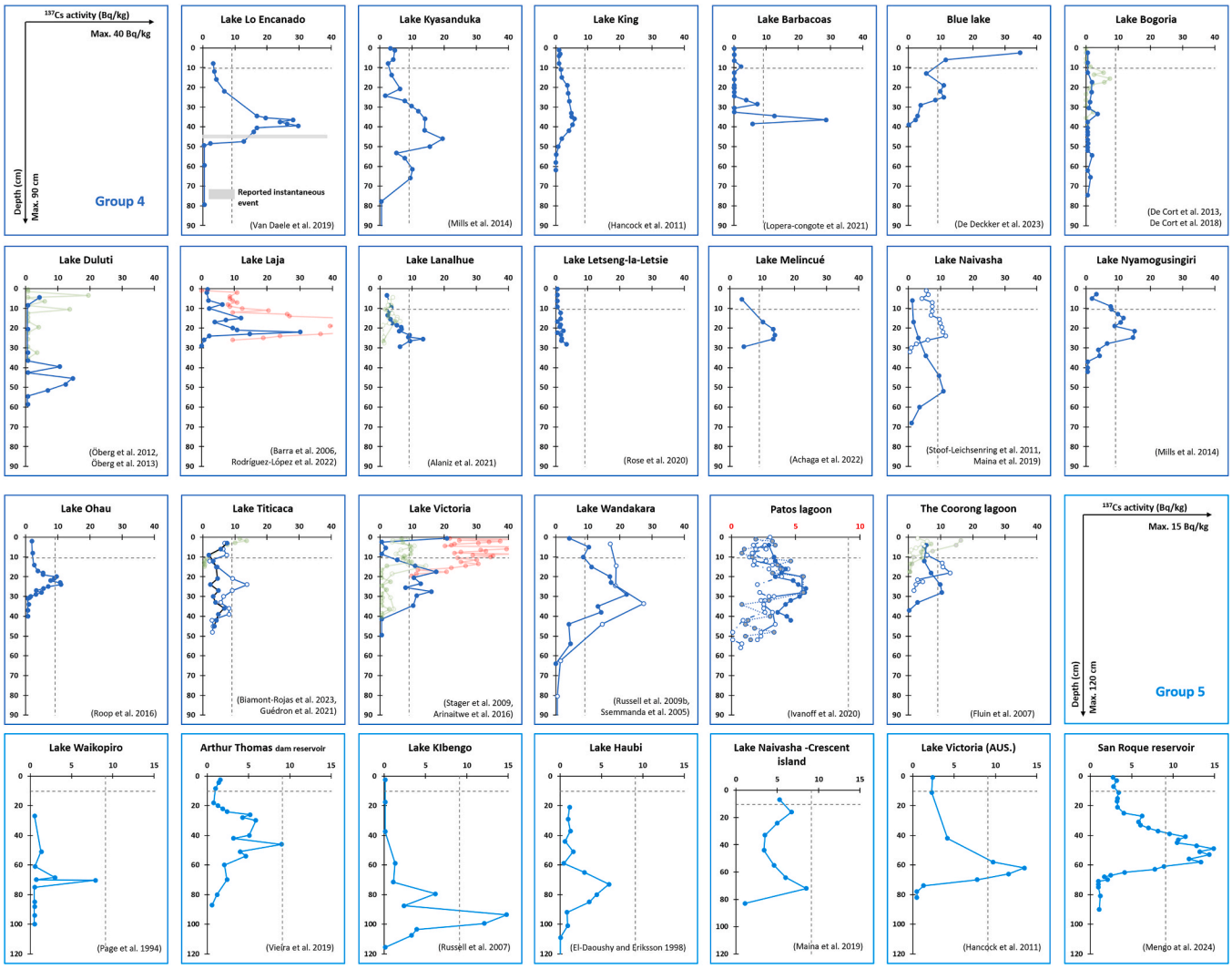

Fig. 5. (*continued*).

cm-yr^{-1}, Table 4). This suggests that increased sediment accumulation may have diluted the ^{137}Cs signal within the sediment profile, making the fallout peak less pronounced. The Group 4 lakes are located primarily between 20° and 30°S latitude, along the eastern coasts of Australia, Brazil and Argentina. Several additional Group 4 lakes are also found at lower elevations near the base of the Rwenzori Mountains in equatorial Africa (Fig. S3), indicating a broader geographic spread across the SH which might possible indicate regionally high sedimentation rates due to unsustainable land use.

Group 5 - Low ^{137}Cs peak activity with very high sedimentation rates

Lakes in Group 5 present a^{137}Cs maximum activity peak (7.4 Bq.kg^{-1}; 6.4–8.9 Bq.kg^{-1}) similar to those in Group 3 and 4, but are characterized by a 2.5 times higher sedimentation rate than Group 4 (1.66 cm.yr^{-1}; 1.33–2.49 cm.yr^{-1}, Table 4), which is the highest among the five groups and 15 times higher than that of Group 1. These high sedimentation rates can explain in part lower ^{137}Cs activity peaks due to dilution by increasing sediment inputs. (Fig. S3).

The spatial distribution of the different ^{137}Cs profile groups suggests a geographic pattern. Lakes classified as Group 1 and Group 2 are predominantly located between 40°S and 50°S in South America, particularly concentrated in southern Chile and Argentina. This hotspot is especially evident when examining the ratio of the ^{137}Cs activity peak to sedimentation rate (Fig. S4), where values above 113 are characteristic of this region. These lakes typically exhibit low sedimentation rates, meaning that a 1 cm sampling resolution may integrate several years to even a decade of sediment accumulation. Despite this, they show elevated ^{137}Cs peak activities, suggesting additional fallout input. In contrast, Group 3 lakes, which share similar sedimentation rates but are located further north in Chile and Argentina, display lower peak activities. Although sedimentation rates and ^{137}Cs activity peaks are high in both Group 4 and Group 5, these groups are statistically distinct, indicating different sedimentation dynamics (Fig. S2). To further explore environmental factors potentially explaining this hotspot, we assessed the influence of climatic and geographic variables on ^{137}Cs peak activity, the ^{137}Cs activity peak to sedimentation rate ratio, and the lake groupings derived from HCPC analysis.

3.4. Relationships to environmental parameters

The variability in ^{137}Cs peak activity across lake sediment profiles is partly explained by the sedimentation rate, where lakes with high sedimentation rates (>0.30 cm yr^{-1}) consistently show low ^{137}Cs peak activity, whereas lakes with lower sedimentation rates exhibit a much broader range of ^{137}Cs peak activities across the SH. To investigate the potential environmental controls on this variability, we applied a range of statistical approaches. First, a Spearman correlation matrix was used to identify potential relationships between ^{137}Cs metrics and environmental variables (Fig. S4). To reduce the influence of sediment accumulation, we computed the ratio of the ^{137}Cs peak activity to the sedimentation rate (based on the depth of the 1964/65 peak) as an

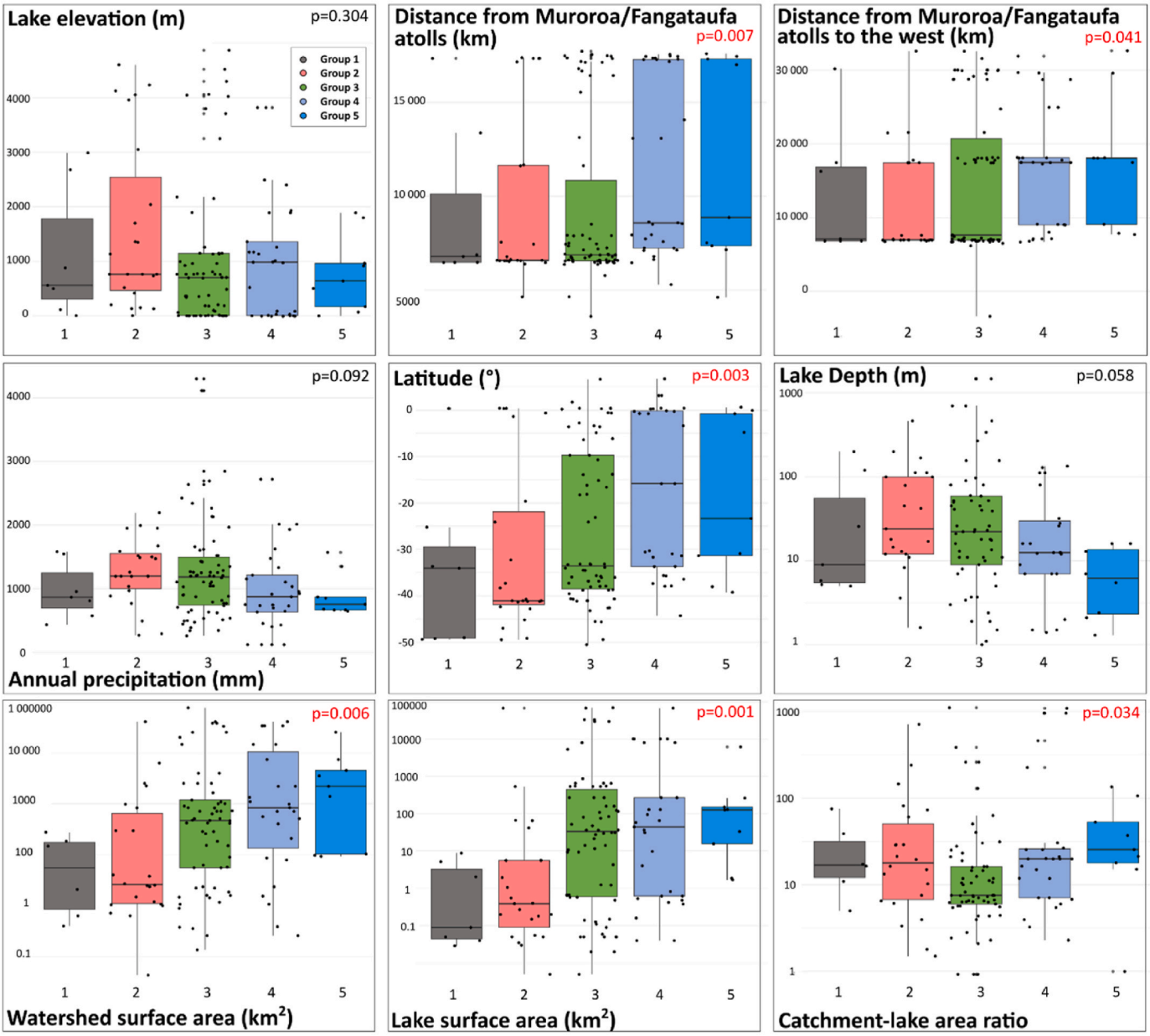

Fig. 6. Boxplots of the different environmental variables across ^{137}Cs profile groups (based on HCPC clustering). Please note that watershed and lake surfaces and catchment to lake ratio areas are expressed in log scale values.

alternative metric (Fig. S5). This ratio helped in normalizing ^{137}Cs activity by the amount of sediment deposited since peak fallout.

No strong direct correlation was found between the ^{137}Cs peak activity or the ^{137}Cs activity sedimentation rate ratio and most of the environmental variables (Fig. S4). The strongest observed correlation was that between latitude and the ^{137}Cs activity peak: sedimentation rate ratio ($R = -0.48$, $p < 0.05$), suggesting that higher ratios (i.e., higher ^{137}Cs peak activity relative to sedimentation rate) are associated with more southern locations (negative latitude).

We also applied multiple linear regression models to identify environmental parameter predictors of ^{137}Cs peak activity and the ratio. These models explained only a small portion of the variance ($R^2 < 0.20$), with geographic variables such as latitude and Euclidean distance from Mururoa emerging as the most significant predictors (Fig. S5). However, the low R^2 value indicates that environmental variables alone are insufficient to fully explain the ^{137}Cs metrics variability.

Similarly, a random forest model was applied to the dataset, but it explained less than 10 % of the variance ($R^2 < 0.1$), indicating a low explanatory power. However, latitude was again identified as one of the most important variables explaining variability in the ^{137}Cs activity peak to sedimentation rate ratio (Fig. S6). Attempts made to restrict the analysis to lakes from South America did not improve model performance.

Given these limitations, we adopted a group comparison approach, in which HCPC-derived profile groups were used to assess whether environmental factors could help to explain differences in ^{137}Cs deposition patterns. Group comparisons revealed significant differences in several environmental parameters (Kruskal-Wallis test) such as the lake surface area ($p = 0.001$), the catchment area ($p = 0.006$), latitude ($p = 0.003$), the Euclidean distance from Mururoa ($p = 0.007$) and the westward distance from Mururoa ($p = 0.04$). Groups 1 and 2 included lakes with the smallest average surface areas and catchment areas, whereas Groups 3, 4, and 5 comprised lakes with larger surface and catchment areas. Lakes with a high catchment-to-lake area ratio are

likely to receive higher sediment input per unit lake area, where ^{137}Cs can be diluted or partially lost, reflecting lower sediment trap efficiency (Pulley et al., 2018; Appleby, 2008). However, the catchment-to-lake area ratio does not clearly distinguish these groups, which might otherwise have explained the differences in sedimentation rate among ^{137}Cs profiles groups (Fig. 6).

Surprisingly, precipitation and elevation did not come out as important predictors of ^{137}Cs peak activity or the ^{137}Cs activity to sedimentation rate ratio. These findings suggest that geographic location, and particularly the distance from the nuclear test sites in French Polynesia, could play a more significant role in the ^{137}Cs deposition patterns. This can be explained by the dominant westerly wind patterns observed between 30° and 50°S that transport fallout across the SH (Chaboche et al., 2022). Evidently, lakes located at latitudes ranging from 40° to 50°S presented the highest ^{137}Cs peak activity.

The variability among profile groups appears to be driven by a combination of geographic factors (especially latitude and distance from Mururoa) and local lake characteristics (notably catchment and lake size). These findings demonstrate the importance of considering both fallout deposition patterns and the catchment settings when interpreting ^{137}Cs profiles.

4. Conclusions and outlook

Despite relatively low ^{137}Cs peak activities in SH lakes compared to the NH, their variability provides valuable insight into hemispheric fallout deposition. On average, ^{137}Cs activity peaks are about seven times lower than those recorded in NH lakes. In some SH regions, ^{137}Cs is below detection limits, but it remains widely measurable and is successfully used to identify the 1964/1965 fallout peak.

To better assess spatial disparities in ^{137}Cs deposition, we examined peak activity normalized by sedimentation rate and used cluster analysis to distinguish lake ^{137}Cs profiles. Five groups emerged, forming a continuum from low peak activity with high sedimentation rates to high peaks with low sedimentation rates. Lakes with the highest ^{137}Cs activity peaks are concentrated between 40°S and 50°S in South America. Neither multiple linear regression nor random forest models showed strong predictive power for environmental drivers of ^{137}Cs peak activity or the ^{137}Cs activity peak to sedimentation rate ratio. However, latitude and distance to nuclear weapon test sites were the most relevant explanatory variables. Compared to lakes with similar sedimentation rates further north, these lakes show higher fallout peak, likely due to their closer proximity to nuclear weapons test sites in the Pacific and exposure to prevailing wind patterns.

Accurate detection of ^{137}Cs peaks requires high resolution sampling and ultra-low background gamma spectrometry, especially in the SH. To enhance inter-lake comparisons and improve understanding of fallout patterns, consistent reporting of dry bulk density is recommended to enable inventory calculations. In South America, a substantial number of ^{137}Cs inventories have been calculated between 35°S and 45°S, showing values in line with expected atmospheric deposition.

As part of the AVATAR project, we initiated a participatory network to study artificial radionuclides (^{137}Cs, ^{239}Pu and ^{240}Pu) in SH lake sediments. We encourage the paleolimnology and environmental science communities to contribute additional or unpublished lake ^{137}Cs data to the ARLASH database (https://doi.org/10.5281/zenodo.15921856). Such initiative will advance global efforts to understand artificial radionuclides deposition in freshwater systems and support more robust sediment dating in the Southern Hemisphere.

CRediT authorship contribution statement

Floriane Guillevic: Writing – original draft, Visualization, Validation, Methodology, Formal analysis, Data curation, Conceptualization. **Pierre Sabatier:** Writing – review & editing, Visualization, Validation, Methodology, Conceptualization. **Gerald Dicen:** Writing – review & editing, Methodology, Conceptualization. **Palak Aggarwal:** Data curation. **Anthony Foucher:** Writing – review & editing, Validation. **Olivier Evrard:** Writing – review & editing, Validation, Funding acquisition. **Christine Alewell:** Writing – review & editing, Validation, Methodology, Funding acquisition, Conceptualization.

Declaration of competing interest

The authors declare the following financial interests/personal relationships which may be considered as potential competing interests: Christine Alewell reports financial support was provided by Swiss National Science Foundation. If there are other authors, they declare that they have no known competing financial interests or personal relationships that could have appeared to influence the work reported in this paper.

Acknowledgments

We thank the two anonymous reviewers for their comments and suggestions which help to improve the clarity of the manuscript as well as the associate editor for the handling of our manuscript. The AVATAR project is funded by the Swiss National Science Foundation (SNSF; grant no. 212886) and the French National Research Agency (ANR; grant no. ANR-22-CE93-0001).

Appendix A. Supplementary data

Supplementary data to this article can be found online at https://doi.org/10.1016/j.jenvrad.2026.107906.

Data availability

The ARLASH Database may be accessed from the Zenodo repository: https://doi.org/10.5281/zenodo.15921856.

The R script used for analysis is available upon request.

References

Aoyama, M., Hirose, K., Igarashi, Y., 2006. Re-construction and updating our understanding on the global weapons tests 137Cs fallout. J. Environ. Monit. 8, 431–438. https://doi.org/10.1039/B512601K.

Appleby, P.G., 2001. Chronostratigraphic techniques in recent sediments. In: Last, W.M., Smol, J.P. (Eds.), Tracking Environmental Change Using Lake Sediments: Basin Analysis, Coring, and Chronological Techniques, Developments in Paleoenvironmental Research. Springer, Netherlands, Dordrecht, pp. 171–203. https://doi.org/10.1007/0-306-47669-X_9.

Appleby, P.G., 2008. Three decades of dating recent sediments by fallout radionuclides: a review. Holocene 18, 83–93. https://doi.org/10.1177/0959683607085598.

Appleby, P.G., Semertzidou, P., Piliposian, G.T., Chiverrell, R.C., Schillereff, D.N., Warburton, J., 2019. The transport and mass balance of fallout radionuclides in brotherswater, Cumbria (UK). J. Paleolimnol. 62, 389–407. https://doi.org/10.1007/s10933-019-00095-z.

Arnaud, F., Magand, O., Chapron, E., Bertrand, S., Boes, X., Charlet, F., Melieres, M.-A., 2006a. Radionuclide dating (Pb-210, Cs-137, Am-241) of recent lake sediments in a highly active geodynamic setting (Lakes Puyehue and Icalma-Chilean Lake District). Sci. Total Environ. 366, 837–850. https://doi.org/10.1016/j.scitotenv.2005.08.013.

Bandowe, B.A.M., Fränkl, L., Grosjean, M., Tylmann, W., Mosquera, P.V., Hampel, H., Schneider, T., 2018. A 150-year record of polycyclic aromatic compound (PAC) deposition from high Andean Cajas national park, southern Ecuador. Sci. Total Environ. 621, 1652–1663. https://doi.org/10.1016/j.scitotenv.2017.10.060.

Bird, B., Rudloff, O., Escobar, J., Gilhooly, W., Correa-Metrio, A., Vélez, M., Polissar, P., 2018. Paleoclimate support for a persistent dry island effect in the Colombian Andes during the last 4700 years. Holocene 28, 217–228. https://doi.org/10.1177/0959683617721324.

Branchu, P., Bergonzini, L., Pons-branchu, E., Violier, E., Dittrich, M., Massault, M., Ghaleb, B., 2010. Lake Malawi sediment and pore water chemistry: proposition of a conceptual model for stratification intensification since the end of the little ice age. Global and Planetary Change, Quaternary and Global Change: Review and Issues Special issue in memory of Hugues FAURE 72, 321–330. https://doi.org/10.1016/j.gloplacha.2010.01.008.

Bruel, R., Sabatier, P., 2020. serac: a R package for ShortlivEd RAdionuclide chronology of recent sediment cores. J. Environ. Radioact. https://doi.org/10.1016/j.jenvrad.2020.106449.

Bueno, C., Sanders, C.J., Niencheski, F.H., Andrade, C., Burnett, W., Santos, I.R., 2021. Organic carbon accumulation in oligotrophic coastal lakes in southern Brazil during the last century. J. Paleolimnol. 66, 71–82. https://doi.org/10.1007/s10933-021-00187-9.

Chaboche, P.-A., Pointurier, F., Sabatier, P., Foucher, A., Tiecher, T., Minella, J.P.G., Tassano, M., Hubert, A., Morera, S., Guédron, S., Ardois, C., Boulet, B., Cossonnet, C., Cabral, P., Cabrera, M., Chalar, G., Evrard, O., 2022. 240Pu/239Pu signatures allow refining the chronology of radionuclide fallout in South America. Sci. Total Environ. 843, 156943. https://doi.org/10.1016/j.scitotenv.2022.156943.

Corcoran, M., Sherif, M.I., Smalley, C., Li, A., Rockne, K.J., Giesy, J.P., Sturchio, N.C., 2018. Accumulation rates, focusing factors, and chronologies from depth profiles of 210Pb and 137Cs in sediments of the Laurentian Great Lakes. J. Gt. Lakes Res. 44, 693–704. https://doi.org/10.1016/j.jglr.2018.05.013.

Daga, R., Ribeiro Guevara, S., Sánchez, M.L., Arribére, M., 2008. Source identification of volcanic ashes by geochemical analysis of well preserved lacustrine tephras in Nahuel Huapi national park. Appl. Radiat. Isot. 66, 1325–1336. https://doi.org/10.1016/j.apradiso.2008.03.009.

Dicen, G., Guillevic, F., Gupta, S., Chaboche, P.-A., Meusburger, K., Sabatier, P., Evrard, O., Alewell, C., 2025. Distribution and sources of fallout ^{137}Cs and $^{239+240}$Pu in equatorial and Southern Hemisphere reference soils. Earth Syst. Sci. Data 17, 1529–1549. https://doi.org/10.5194/essd-17-1529-2025.

Edgington, D.N., Robbins, J.A., 1990. Time scales of sediment focusing in large Lakes as revealed by measurement of fallout Cs-137. In: Tilzer, M.M., Serruya, C. (Eds.), Large Lakes: Ecological Structure and Function. Springer, Berlin, Heidelberg, pp. 210–223. https://doi.org/10.1007/978-3-642-84077-7_11.

Evrard, O., Chaboche, P.-A., Ramon, R., Foucher, A., Laceby, J.P., 2020. A global review of sediment source fingerprinting research incorporating fallout radiocesium (137Cs). Geomorphology 362, 107103. https://doi.org/10.1016/j.geomorph.2020.107103.

Ficetola, G.F., Poulenard, J., Sabatier, P., Messager, E., Gielly, L., Leloup, A., Etienne, D., Bakke, J., Malet, E., Fanget, B., Støren, E., Reyss, J.-L., Taberlet, P., Arnaud, F., 2018. DNA from lake sediments reveals long-term ecosystem changes after a biological invasion. Sci. Adv. 4, eaar4292. https://doi.org/10.1126/sciadv.aar4292.

Foucher, A., Chaboche, P.-A., Sabatier, P., Evrard, O., 2021. A worldwide meta-analysis (1977–2020) of sediment core dating using fallout radionuclides including ^{137}Cs and ^{210}Pb$_{xs}$. Earth Syst. Sci. Data 13, 4951–4966. https://doi.org/10.5194/essd-13-4951-2021.

Foucher, A., Tassano, M., Chaboche, P.-A., Chalar, G., Cabrera, M., Gonzalez, J., Cabral, P., Simon, A.-C., Agelou, M., Ramon, R., Tiecher, T., Evrard, O., 2023. Inexorable land degradation due to agriculture expansion in South American Pampa. Nat. Sustain. 6, 662–670. https://doi.org/10.1038/s41893-023-01074-z.

Frugone-Alvarez, M., Latorre, C., Giralt, S., Polanco-Martinez, J., Bernardez, P., Oliva-Urcia, B., Maldonado, A., Laura Carrevedo, M., Moreno, A., Delgado Huertas, A., Prego, R., Barreiro-Lostres, F., Valero-Garces, B., 2017. A 7000-year high-resolution lake sediment record from coastal central Chile (Lago Vichuquen, 34 degrees S): implications for past sea level and environmental variability. J. Quat. Sci. 32, 830–844. https://doi.org/10.1002/jqs.2936.

Garcia-Rodriguez, F., Mazzeo, N., Sprechmann, P., Metzeltin, D., Sosa, F., Treutler, H., Renom, M., Scharf, B., Gaucher, C., 2002. Paleolimnological assessment of human impacts in Lake Blanca, SE Uruguay. J. Paleolimnol. 28, 457–468. https://doi.org/10.1023/A:1021616811341.

Godoy, J.M., Padovani, C.R., Guimarães, J.R.D., Pereira, J.C.A., Vieira, L.M., Carvalho, Z. L., Galdino, S., 2002. Evaluation of the siltation of river Taquari, pantanal, Brazil, through 210Pb geochronology of floodplain Lake sediments. J. Braz. Chem. Soc. 13, 71–77. https://doi.org/10.1590/S0103-50532002000100011.

Guédron, S., Tolu, J., Delaere, C., Sabatier, P., Barre, J., Heredia, C., Brisset, E., Campillo, S., Bindler, R., Fritz, S.C., Baker, P.A., Amouroux, D., 2021. Reconstructing two millennia of copper and silver metallurgy in the Lake Titicaca region (Bolivia/Peru) using trace metals and lead isotopic composition. Anthropocene 34, 100288. https://doi.org/10.1016/j.ancene.2021.100288.

Guilizzoni, P., Massaferro, J., Lami, A., Luis Piovano, E., Ribeiro Guevara, S., Maris Formica, S., Daga, R., Rizzo, A., Gerli, S., 2009. Palaeolimnology of Lake Hess (Patagonia, Argentina): multi-proxy analyses of short sediment cores. Hydrobiologia 631, 289–302. https://doi.org/10.1007/s10750-009-9818-5.

Hancock, G.J., Leslie, C., Everett, S.E., Tims, S.G., Brunskill, G.J., Haese, R., 2011. Plutonium as a chronomarker in Australian and New Zealand sediments: a comparison with 137Cs. J. Environ. Radioact. 102, 919–929. https://doi.org/10.1016/j.jenvrad.2009.09.008.

He, Q., Walling, D.E., 1997. The distribution of fallout 137Cs and 210Pb in undisturbed and cultivated soils. Appl. Radiat. Isot. 48, 677–690. https://doi.org/10.1016/S0969-8043(96)00302-8.

He, Q., Walling, D.E., Owens, P.N., 1996. Interpreting the 137Cs profiles observed in several small lakes and reservoirs in southern England. Chem. Geol. 129, 115–131. https://doi.org/10.1016/0009-2541(95)00149-2.

Health and Safety Laboratory, 1977. Health and safety laboratory environmental quarterly. Final Tabulation of Monthly/sup 90/Sr Fallout Data: 1954–1976 (Report No. HASL-329). Energy Research and Development Administration, New York (USA). Health and Safety Lab.

Hijmans, R.J., Cameron, S.E., Parra, J.L., Jones, P.G., Jarvis, A., 2005. Very high resolution interpolated climate surfaces for global land areas. Int. J. Climatol. 25, 1965–1978. https://doi.org/10.1002/joc.1276.

Jagercikova, M., Cornu, S., Le Bas, C., Evrard, O., 2015. Vertical distributions of 137Cs in soils: a meta-analysis. J. Soils Sediments 15, 81–95. https://doi.org/10.1007/s11368-014-0982-5.

Josse, J., Husson, F., 2016. missMDA: a package for handling missing values in multivariate data analysis. J. Stat. Software 70, 1–31. https://doi.org/10.18637/jss.v070.i01.

Ketterer, M.E., Hafer, K.M., Jones, V.J., Appleby, P.G., 2004. Rapid dating of recent sediments in Loch Ness: inductively coupled plasma mass spectrometric measurements of global fallout plutonium. Sci. Total Environ. 322, 221–229. https://doi.org/10.1016/j.scitotenv.2003.09.016.

Lê, S., Josse, J., Husson, F., 2008. FactoMineR: an R package for multivariate analysis. J. Stat. Software 25, 1–18. https://doi.org/10.18637/jss.v025.i01.

Ledru, M.-P., Jeske-Pieruschka, V., Bremond, L., Develle, A.-L., Sabatier, P., Martins, E.S. P.R., de Freitas Filho, M.R., Fontenele, D.P., Arnaud, F., Favier, C., Barroso, F.R.G., Araújo, F.S., 2020. When archives are missing, deciphering the effects of public policies and climate variability on the Brazilian semi-arid region using sediment core studies. Sci. Total Environ. 723, 137989. https://doi.org/10.1016/j.scitotenv.2020.137989.

Mackay, A.W., Lee, R., Russell, J.M., 2021. Recent climate-driven ecological changes in tropical montane lakes of Rwenzori Mountains national park, Central Africa. J. Paleolimnol. 65, 219–234. https://doi.org/10.1007/s10933-020-00161-x.

MacKenzie, A.B., Farmer, J.G., Sugden, C.L., 1997. Isotopic evidence of the relative retention and mobility of lead and radiocaesium in Scottish ombrotrophic peats. Sci. Total Environ. 203, 115–127. https://doi.org/10.1016/S0048-9697(97)00139-3.

McCarthy, F.M., Patterson, R.T., Head, M.J., Riddick, N.L., Cumming, B.F., Hamilton, P. B., Pisaric, M.F., Gushulak, A.C., Leavitt, P.R., Lafond, K.M., Llew-Williams, B., Marshall, M., Heyde, A., Pilkington, P.M., Moraal, J., Boyce, J.I., Nasser, N.A., Walsh, C., Garvie, M., Roberts, S., Rose, N.L., Cundy, A.B., Gaca, P., Milton, A., Hajdas, I., Crann, C.A., Boom, A., Finkelstein, S.A., McAndrews, J.H., 2023. The varved succession of Crawford Lake, Milton, Ontario, Canada as a candidate global boundary stratotype section and point for the anthropocene series. Anthropol. Rev. 10, 146–176. https://doi.org/10.1177/20530196221149281.

Messager, M.L., Lehner, B., Grill, G., Nedeva, I., Schmitt, O., 2016. Estimating the volume and age of water stored in global lakes using a geo-statistical approach. Nat. Commun. 7, 13603. https://doi.org/10.1038/ncomms13603.

Meusburger, K., Evrard, O., Alewell, C., Borrelli, P., Cinelli, G., Ketterer, M., Mabit, L., Panagos, P., van Oost, K., Ballabio, C., 2020. Plutonium aided reconstruction of caesium atmospheric fallout in European topsoils. Sci. Rep. 10, 11858. https://doi.org/10.1038/s41598-020-68736-2.

Michelutti, N., Lemmen, J.L., Cooke, C.A., Hobbs, W.O., Wolfe, A.P., Kurek, J., Smol, J. P., 2016. Assessing the effects of climate and volcanism on diatom and chironomid assemblages in an Andean Lake near Quito, Ecuador. J. Limnol. 75, 275–286. https://doi.org/10.4081/jlimnol.2015.1323.

Michelutti, N., Sowell, P., Tapia, P.M., Grooms, C., Polo, M., Gambetta, A., Ausejo, C., Smol, J.P., 2019. A pre-Inca pot from underwater ruins discovered in an Andean lake provides a sedimentary record of marked hydrological change. Sci. Rep. 9. https://doi.org/10.1038/s41598-019-55422-1.

Pasche, N., Alunga, G., Mills, K., Muvundja, F., Ryves, D.B., Schurter, M., Wehrli, B., Schmid, M., 2010. Abrupt onset of carbonate deposition in Lake Kivu during the 1960s: response to recent environmental changes. J. Paleolimnol. 44, 931–946. https://doi.org/10.1007/s10933-010-9465-x.

Pennington, W., Tutin, T.G., Cambray, R.S., Fisher, E.M., 1973. Observations on Lake sediments using fallout 137Cs as a tracer. Nature 242, 324–326. https://doi.org/10.1038/242324a0.

Pulley, S., Foster, I.D.L., Collins, A.L., Zhang, Y., Evans, J., 2018. An analysis of potential controls on long-term 137Cs accumulation in the sediments of UK lakes. J. Paleolimnol. 60, 1–30. https://doi.org/10.1007/s10933-017-0016-6.

R Core Team, 2024. _R: a Language and Environment for Statistical Computing_. R Foundation for Statistical Computing, Vienna, Austria. https://www.R-project.org/.

Reyss, J.-L., Schmidt, S., Legeleux, F., Bonté, P., 1995. Large, low background well-type detectors for measurements of environmental radioactivity. Nucl. Instrum. Methods Phys. Res. Sect. Accel. Spectrometers Detect. Assoc. Equip. 357, 391–397. https://doi.org/10.1016/0168-9002(95)00021-6.

Ribeiro Guevara, S., Arribére, M., 2002. 137Cs dating of lake cores from the Nahuel Huapi national park, Patagonia, Argentina: historical records and profile measurements. J. Radioanal. Nucl. Chem. 252, 37–45. https://doi.org/10.1023/A:1015275418412.

Ritchie, J.C., McHenry, J.R., 1990. Application of radioactive fallout Cesium-137 for measuring soil erosion and sediment accumulation rates and patterns: a review. J. Environ. Qual. 19, 215–233. https://doi.org/10.2134/jeq1990.00472425001900020006x.

Ritchie, J.C., McHenry, J.R., Gill, A.C., 1973. Dating recent reservoir sediments. Limnol. Oceanogr. 18, 254–263.

Rohatgi, A., 2015. WebPlotDigitizer. WebPlotDigitizer Online Software (Version 5.1) [Computer software].

Röllin, S., Corcho-Alvarado, J.A., Sahli, H., Putyrskaya, V., Klemt, E., 2022. High-resolution records of cesium, plutonium, americium, and uranium isotopes in sediment cores from Swiss lakes. Environ. Sci. Pollut. Res. https://doi.org/10.1007/s11356-022-20785-y.

Rose, N.L., Turner, S.D., Unger, L.E., Curtis, C.J., 2021. The chronostratigraphy of the anthropocene in Southern Africa: current status and potential. SOUTH Afr. J. Geol. 124, 1093–1106. https://doi.org/10.25131/sajg.124.0053.

Sanders, L.M., Taffs, K.H., Stokes, D., Enrich-Prast, A., Sanders, C.J., 2017. Pu240+239 DEPOSITIONAL SIGNATURES AS A VIABLE GEOCHRONOLOGICAL TOOL IN THE AMAZON BASIN. Geochronometria 44, 142–149. https://doi.org/10.1515/geochr-2015-0068.

Saunders, K.M., Kamenik, C., Hodgson, D.A., Hunziker, S., Siffert, L., Fischer, D., Fujak, M., Gibson, J.A.E., Grosjean, M., 2012. Late Holocene changes in precipitation in northwest Tasmania and their potential links to shifts in the Southern Hemisphere

westerly winds. Global Planet. Change 92–93, 82–91. https://doi.org/10.1016/j.gloplacha.2012.04.005.

Stager, J.C., Hecky, R.E., Grzesik, D., Cumming, B.F., Kling, H., 2009. Diatom evidence for the timing and causes of eutrophication in Lake Victoria, East Africa. Hydrobiologia 636, 463–478. https://doi.org/10.1007/s10750-009-9974-7.

Strother, S.L., Salzmann, U., Roberts, S.J., Hodgson, D.A., Woodward, J., Van Nieuwenhuyze, W., Verleyen, E., Vyverman, W., Moreton, S.G., 2015. Changes in Holocene climate and the intensity of Southern Hemisphere westerly winds based on a high-resolution palynological record from sub-Antarctic South Georgia. Holocene 25, 263–279. https://doi.org/10.1177/0959683614557576.

Thomson, J., Dyer, F.M., Croudace, I.W., 2002. Records of radionuclide deposition in two salt marshes in the United Kingdom with contrasting redox and accumulation conditions. Geochem. Cosmochim. Acta 66, 1011–1023. https://doi.org/10.1016/S0016-7037(01)00825-0.

UNSCEAR (United Nations Scientific Committee on the Effects of Atomic Radiation), 2000. Sources and effects of ionizing radiation. In: UNSCEAR 2000 Report to the General Assembly, with Scientific Annexes, vol. I. United Nations, New York.

Walling, D.E., Qingping, H., 1992. Interpretation of caesium-137 profiles in lacustrine and other sediments: the role of catchment-derived inputs. Hydrobiologia 235, 219–230. https://doi.org/10.1007/BF00026214.

Weisbrod, B., Wood, S.A., Steiner, K., Whyte-Wilding, R., Puddick, J., Laroche, O., Dietrich, D.R., 2020. Is a central sediment sample sufficient? Exploring spatial and temporal microbial diversity in a small Lake. Toxins 12, 580. https://doi.org/10.3390/toxins12090580.

Wils, K., Daryono, M., Praet, N., Santoso, A., Dianto, A., Schmidt, S., Vervoort, M., Huang, J., Kusmanto, E., Suandhi, P., Natawidjaja, D., De Batist, M., 2021a. The sediments of Lake Singkarak and Lake Maninjau in West Sumatra reveal their earthquake, volcanic and rainfall history. Sediment. Geol. 416. https://doi.org/10.1016/j.sedgeo.2021.105863.

Zalles, V., Hansen, M.C., Potapov, P.V., Parker, D., Stehman, S.V., Pickens, A.H., Parente, L.L., Ferreira, L.G., Song, X.-P., Hernandez-Serna, A., Kommareddy, I., 2021. Rapid expansion of human impact on natural land in South America since 1985. Sci. Adv. 7. https://doi.org/10.1126/sciadv.abg1620 eabg1620.

Zhao, X., Hou, X., Zhou, W., Lei, D., Han, Y., Yan, D., Jiang, H., An, Z., 2025. Plutonium marker for the great acceleration by intensified human activities. Environ. Sci. Technol. https://doi.org/10.1021/acs.est.4c11841.